Surface plasmon polaritons on narrow-ridged short-pitch metal gratings in the conical mount

Ian R. Hooper and J. R. Sambles

Thin Film Photonics Group, School of Physics, University of Exeter, Stocker Road, Exeter, EX4 4QL, UK

Received September 16, 2002; revised manuscript received December 2, 2002; accepted December 4, 2002

Recent investigations into high-aspect-ratio short-pitch metal grating structures have shown that it is possible to excite surface plasmon polaritons (SPPs) even in the zero-order region of the spectrum. The predominant reason this is possible is that extremely large bandgaps occur in the SPP dispersion curves, which are caused by the large depths, and heights, of the structures. The form of the resultant dispersion curves has also been found to be highly dependent on the shape of the grating profile. We present an extension to a previously published paper that described the nature of the SPPs excited on narrow-ridged short-pitch metal gratings in the classical mount by considering the case in which the radiation is incident at nonzero azimuthal angles (the conical mount). In particular, we consider the case of 90° and 45° azimuthal angles and discuss the coupling to the SPP modes and the way in which polarization conversion is evident on such structures.

OCIS code: 050.1950.

1. INTRODUCTION

The surface plasmon polariton (SPP) is an electromagnetic (EM) surface excitation at a metal–dielectric interface, which consists of a surface-charge-density oscillation coupled to EM fields.[1] Owing to the necessary wave-vector-matching condition needed for excitation of a SPP, it is not possible to excite one on a planar metal–dielectric interface without some method of increasing the wave vector of the incident EM radiation. One method of achieving this is to periodically pattern the interface with a grating structure, and resonant absorption of the incident EM radiation can then occur when the SPP is excited. The shape and period of the corrugation define the shape and position in ω–k space of the resonant absorption, and therefore, by controlling the form of the grating, the optical response of the structure can be closely controlled, permitting surfaces with specific optical responses to be designed.

The change in the optical response of shallow gratings due to the excitation of SPPs is well understood and has been studied for many years. Recent advances in computational power and in the development of manufacturing techniques capable of producing high-aspect-ratio submicrometer structures have stimulated interest in gratings with high aspect ratios (where the depth of the grating is of the order of, or greater than, the grating pitch).

It has been found experimentally that deep lamellar gratings can support highly localized resonances within the grooves with grating pitches (λg) of 1.75 μm and depths of up to 1 μm.[2,3] These flat-banded resonances are very different from SPPs on shallow gratings and have been explained as being due to hybrid waveguide–SPP resonances. An extension of the studies on deep gratings evaluated the band structures for lamellar transmission gratings with a pitch of 3.5 μm and a depth of 4 μm.[4] These also showed flat-banded resonances in the infrared region of the spectrum and predicted almost total resonant transmittance of the incident light upon excitation of the SPP. Other recent developments have shown that resonantly enhanced optical transmission can take place through hole arrays in classically opaque metal films,[5,6] which is also associated with SPP excitation.[7,8]

The majority of the work described has related to diffractive, high-aspect-ratio structures. Until recently it had been assumed that, if the corrugation has a pitch less than half the wavelength of the incident radiation (in other words, it is zero order, or nondiffractive), the interface would act as a good mirror. The reason for this is that, besides having no available diffracted orders, it was thought that SPPs would no longer be excited, since, even with the added wave vector available to the incident radiation owing to scattering from the grating, the wave vectors of the SPPs on such a structure are greater than the photon wave vectors available to the radiation in the zero-order region of the spectrum. However, it has now been shown that, for very deep and narrow-grooved zero-order monogratings, the SPP dispersion curve may be so severely modified from the shallow grating case that resonant absorption of light due to SPP excitation may occur within the zero-order region of the spectrum.[9–11] A family of these resonances has been demonstrated to exist, and these have been termed self-coupled SPP resonances. They are flat banded, possessing near zero group velocity over a large range of incident wave vectors.

Work has also been performed on zero-order narrow-ridged metal gratings in the classical mount, which has also shown that SPPs may be excited in the zero-order region of the spectrum.[12] The dispersion of these SPP modes with changing in-plane wave vector is very different from the narrow-grooved structures and is rather more complex (see Figs. 2 and 7 in Ref. 12). This complex dispersion has been shown to arise from the formation of very large bandgaps in the SPP dispersion curves and through interactions between different SPP bands. The

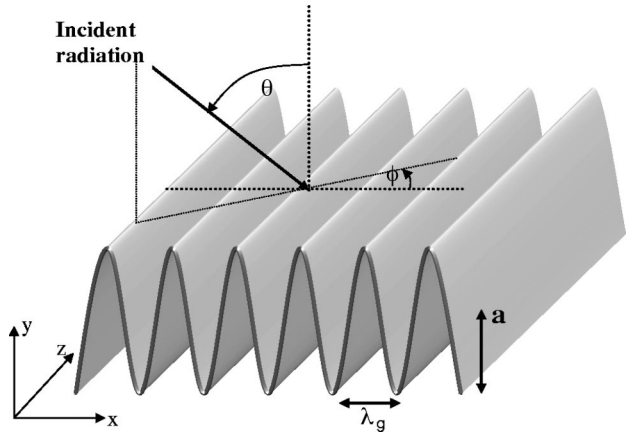

Fig. 1. Schematic of the system under consideration showing the angles used to define the grating orientation with respect to the incident light and the coordinate system.

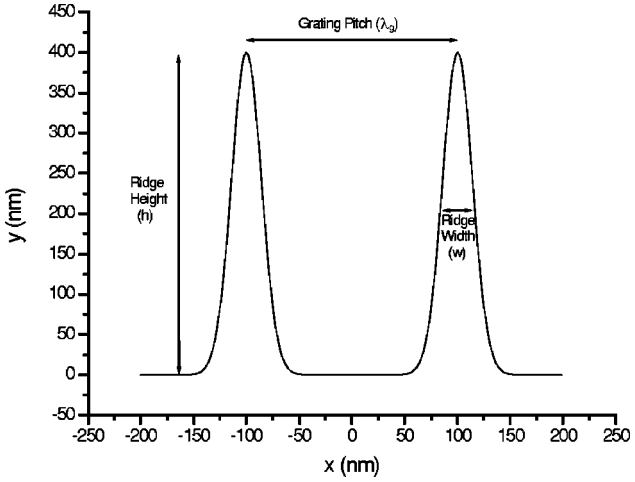

Fig. 2. Schematic of the type of grating profile used in this paper. The grating is described as a series of Gaussian ridges that are defined by their height and width (FWHM).

nature of the SPP modes (at near-normal incidence) is that they are standing waves with an antisymmetric surface charge distribution on either side of the grating ridges.

In this paper we shall extend the study of these narrow-ridged gratings to consider the case where the grating is in the conical mount and, in particular, at azimuthal angles of 90° and 45° (a schematic of the system under consideration that demonstrates the two angles needed to define the grating orientation with respect to the incident light—the polar and azimuthal angles—and the coordinate system used is shown in Fig. 1). When the azimuthal angle is 90° we will show that the low-energy bands produced by bandgaps in the SPP dispersion curves may be excited only with TM-polarized light (the plane of polarization is in the plane of incidence) and describe how the coupling to the mode with this polarization arises. Similarly, the high-energy bands may be coupled to by TE-polarized light only (the plane of polarization is perpendicular to the plane of incidence). We will also explain the dispersion of these modes in terms of anticrossing between the SPP dispersion curves created by scattering from the grating and the planar surface branch of the SPP dispersion curve arising from the origin, which is relatively unperturbed by the grating.

When the grating is oriented at a 45° azimuthal angle, polarization conversion can occur. In fact, there is a mechanism that produces broadband polarization conversion on these structures (which is discussed in a separate paper[13]), and the consequence of exciting the SPPs is to either enhance or suppress the polarization conversion, depending on whether or not the SPP occurs in a region of this broadband polarization conversion. We shall also give a brief description of the dispersion of the modes in this orientation.

2. COMPUTATIONAL METHOD

The method used to obtain the theoretical modeling presented here has been reported extensively elsewhere[14] and is based on a formalism originally proposed by Chandezon *et al.*[15] This is a differential method, utilizing a nonorthogonal curvilinear coordinate transformation to map the grating profile onto a flat plane. This allows easier matching of the boundary conditions, though it does produce a more complex form of Maxwell's equations. A scattering matrix for the system is obtained, from which the reflectivities are calculated. By identifying peaks in the scattering matrices in $\omega-k$ space, we can also obtain the dispersion curves of the modes of the system for all values of $\omega-k$. (In this paper k is split into two orthogonal components to describe the wave vector of the incident light in the plane containing the grating, denoted k_x and k_z for the directions perpendicular and parallel to the grating grooves, respectively.)

In all of the following, the grating profile is described by a series of Gaussian ridges, which permits the width and height of the ridges to be altered independently. In this study the grating pitch is always 200 nm, and the ridge widths are 40 nm. An example of the type of profile investigated is shown in Fig. 2. In explaining some of the phenomena later in this paper, we will describe the grating in terms of its harmonic content and the harmonics in terms of multiples of the grating vector, k_g, where $k_g = 2\pi/\lambda_g$. The permittivity of the metal gratings is modeled as that of silver and is described by a Drude model with a plasma frequency of $\omega_p = 1.32 \times 10^{16}\,\mathrm{s}^{-1}$ and a relaxation time of $\tau = 1.45 \times 10^{-14}\,\mathrm{s}$.

3. SURFACE PLASMON POLARITONS ON NARROW-RIDGED SHORT-PITCH METAL GRATINGS AT A 90° AZIMUTHAL ANGLE

An SPP excited by TM-polarized light on deep metal gratings oriented at a 90° azimuthal angle was first discovered by Watts *et al.*[16] In the results presented in this section these modes will be evident, and we shall discuss why this mode is excited on these narrow-ridged structures and not on the narrow-grooved structures that have been studied previously. We shall also describe the dispersion of these modes with changing in-plane wave vector.

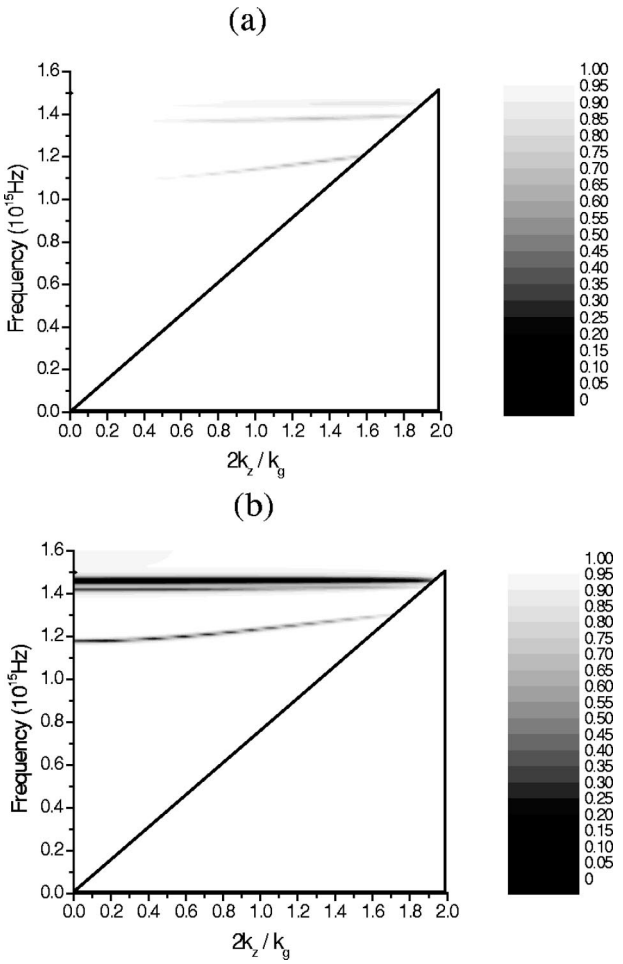

Fig. 3. Zero-order reflectivity from a 200-nm-pitch silver grating consisting of a series of 10-nm-deep, 40-nm-wide Gaussian ridges, oriented at a 90° azimuthal angle, as a function of frequency and in-plane wave vector. (a) TM-polarized radiation, (b) TE-polarized radiation.

The zero-order reflectivity as a function of frequency and in-plane wave vector for a 200-nm-pitch silver grating consisting of 10-nm-deep and 40-nm-wide Gaussian ridges and for an azimuthal angle of 90° is shown in Fig. 3 for both TM- and TE-polarized light. It is important to note at this stage that for this gray-scale plot (and for all subsequent gray-scale plots in this paper) the reflectivity is shown on the z axis, with white indicating high reflectivity and black indicating low reflectivity.

Whether a SPP mode may be coupled to by incident light depends on the symmetry of the surface charges with respect to the grating profile and on the orientation of the electric fields of the incident radiation relative to these surface charges. It is well known that a component of the incident radiation normal to the grating surface is required for coupling to a SPP mode to occur. However, depending on the symmetry of the surface charges, it is not always possible to excite a SPP even if this is the case.

SPP modes may have either symmetric or antisymmetric charge distributions on either side of the grating ridges (for normal incidence), and which type of charge distribution the SPP mode in question consists of is determined by the higher harmonics used to describe the grating profile. These higher harmonics open bandgaps in the SPP dispersion curves, and the two band edges of the bandgap (the low- and high-energy branches, as they will be described here) have different charge symmetries: one with a symmetric charge distribution on either side of the grating ridges, and one with an antisymmetric charge distribution.[13,17] Which of these branches has which charge distribution depends on the sign of the $2k_g$ component of the grating profile (in other words, whether it is $\pm 90°$ with respect to the fundamental component of the Fourier series describing the grating profile). In the case of a Gaussian-ridged grating, the $2k_g$ component of the grating profile is such that the low-energy branch has a symmetric charge distribution and the high-energy branch has an antisymmetric charge distribution.

To explain why incident light may couple only to certain of these modes, we shall consider the example of a Gaussian-ridged grating oriented in the classical mount. In this situation, normally incident TM-polarized light is not able to couple to the low-energy branches of the bandgaps, since the fields of the exciting radiation always point in the same direction (in the direction of the grating vector) for some value of y (normal to the average plane of the grating) and can therefore excite only an antisymmetric charge distribution mode, which in this case is the high-energy branch at the bandgap. However, for nonnormal angles of incidence, this is no longer the case, and coupling may occur to both branches as the field of the incident light will no longer always point in the same direction for some value of y.

It is typically believed that if the azimuthal angle is 90°, TE-polarized light, but not TM-polarized light, may couple to SPP modes. This is not necessarily the case, and it depends on the sign of the $2k_g$ component. For these Gaussian-ridged gratings, TE-polarized light is not able to couple to the low-energy branches at the bandgaps, since only modes with nonsymmetric charge distributions may be excited by it (for the same reasons that TM-polarized light may not couple to the modes at normal incidence in the classical mount). However, unlike the case of TM-polarized light incident on the grating in the classical mount, TE-polarized light may not excite the mode for any polar angle of incidence. Conversely, TM-polarized light may excite the low-energy SPP modes, since its **E** field (for nonnormal polar angles) has a normal component to the surface and will always point in the same direction for all points on the surface at a particular value of y. Since the sign of the $2k_g$ component of the grating profile is the opposite for the case of the Gaussian-grooved structures discussed in Ref. 11, the SPP modes at an azimuthal angle of 90° cannot be excited (since the charge symmetries are reversed as described above).

An additional requirement for the coupling of TM-polarized light to these SPP modes is that the fields of the incident light must point in opposite directions at different points on the surface in the y direction. This is because the surface charge distribution changes sign in the y direction, and this requirement suggests that maximum coupling to the mode will occur when the y component of the wave vector of the incident light is equal to the y component of the SPP wave vector. Of course, this maximum coupling is likely to mean that the mode is overcoupled

and will not result in the lowest reflectivity minimum possible, but it is clear from this argument that the coupling to the mode will increase for higher values of k_z and be very weak for angles near normal incidence. This can clearly be seen from Fig. 4(a) where the coupling to the first-order SPP increases as k_z is increased.

If the height of the grating is increased, then the y component of the SPP wave vector also increases, and therefore, for higher-ridged gratings, the coupling to the SPP will be stronger for lower values of k_z. This is clearly seen if we calculate the same plots as in Fig. 4(a) but for increasing grating depths [Figs. 4(b)–4(d)].

If we investigate the field distributions of these modes, we can show their nature. The $|\mathbf{H}_z|$ component of the fields (the component along the grooves) of the four lowest-energy modes on the structure described for Fig. 4(c), and with $k_z = 0.4$, are shown in Fig. 5.

When the field distributions of Fig. 5 are compared with those of the SPP modes excited in the classical mount (see Fig. 3 in Ref. 12) it is clear that the modes arise from the same origin and correspond to an antisymmetric surface charge distribution on either side of a grating ridge. The main difference between the modes is that, even though the SPPs at a 90° azimuthal angle are standing waves in the x direction (similar to those for the classical mount), they are also propagating in the z direction (and the SPPs excited in the classical mount are not). This can be shown by plotting the field distribution in the x–z plane through one of the SPP field maxima shown in Fig. 5. This has been done for the SPP mode shown in Fig. 5(c) at $y = 110$ nm (through the middle-field maximum) and is shown in Fig. 6.

It is clear, therefore, that the modes are produced by two SPPs propagating at angles to the grating grooves, with one propagating in the $+x$ and $+z$ directions and one propagating in the $-x$ and $+z$ directions, so that the resulting mode is a standing wave in the x direction, propagating in the z direction. The periodicity of the fields in the z direction shown in Fig. 5 is determined by the propagation angle of the SPPs with respect to the grating grooves.

Other features to note in the plots of Fig. 4 are the different dispersion with changing in-plane wave vector of the lowest-energy SPP mode when compared with the higher-order modes and also the anticrossing between this lowest-energy SPP mode and the higher-order SPP modes.

The charge distributions of the low-energy branches of the SPP dispersion curves for these Gaussian-ridged gratings have symmetrical charge distributions on either side of the ridges and therefore have their maximum surface charge densities at the peaks and troughs of the grating

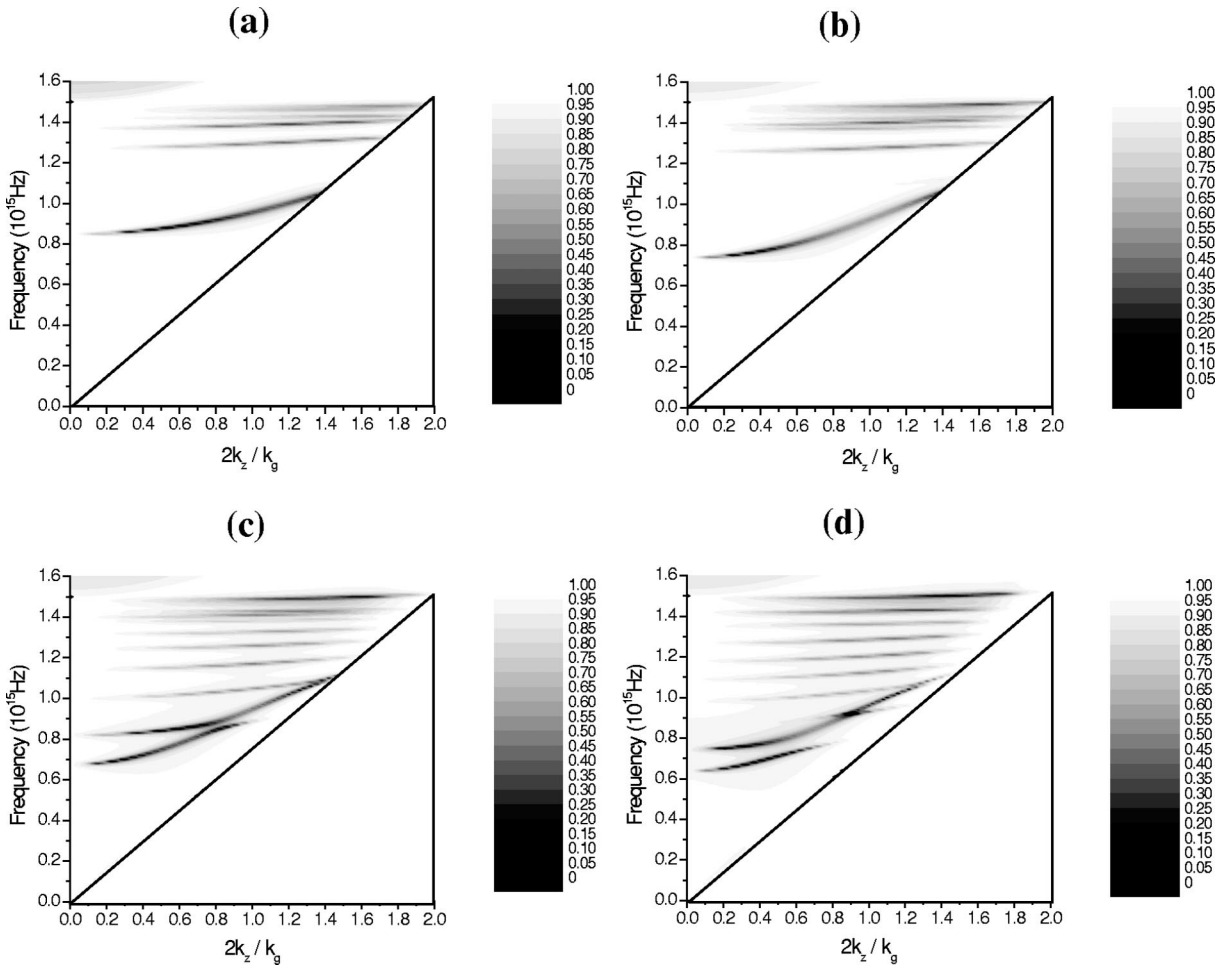

Fig. 4. TM reflectivity from 200-nm-pitch silver gratings consisting of a series of 40-nm-wide Gaussian ridges, oriented at a 90° azimuthal angle, as a function of frequency and in-plane wave vector. (a) $d = 50$ nm, (b) $d = 100$ nm, (c) $d = 200$ nm, (d) $d = 300$ nm.

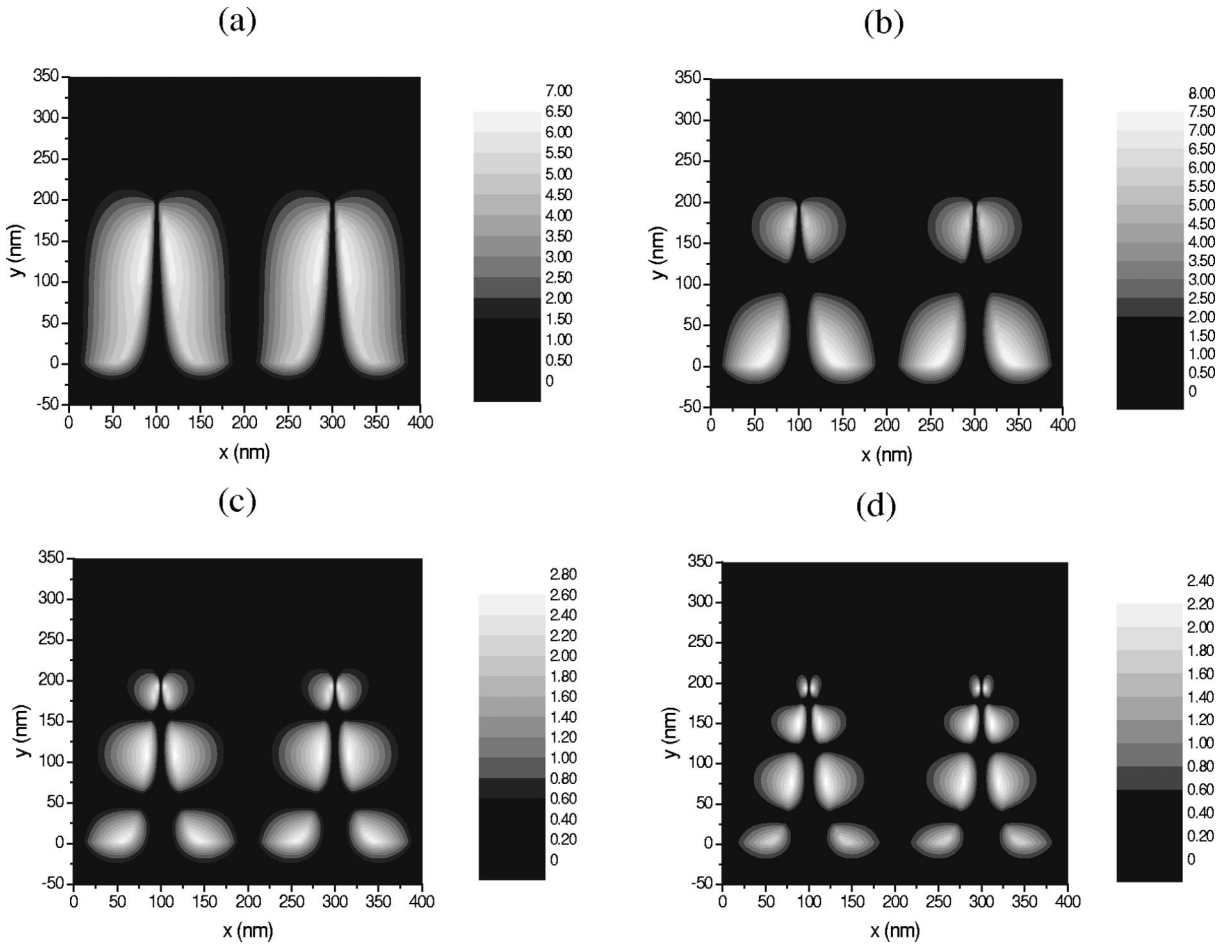

Fig. 5. $|\mathbf{H}_z|$ component of the fields (the component along the grooves) of the four lowest-energy modes on the structure described for Fig. 4(c) and with $k_z = 0.4$. (a) $f = 0.721 \times 10^{15}$ Hz, (b) $f = 0.833 \times 10^{15}$ Hz, (c) $f = 1.008 \times 10^{15}$ Hz, (d) $f = 1.148 \times 10^{15}$ Hz.

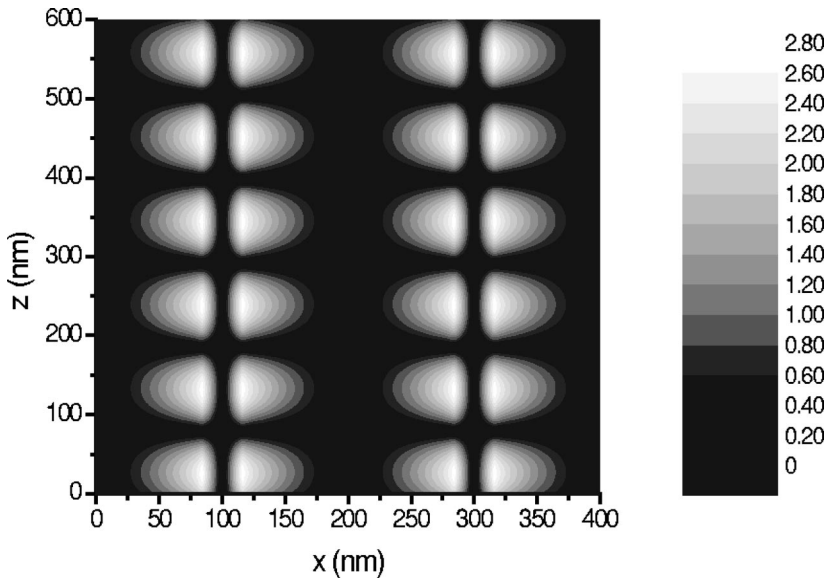

Fig. 6. $|\mathbf{H}_z|$ component of the fields in the x–z plane through the middle-field maximum shown in Fig. 5(c) ($y = 110$ nm).

profile. Since the flat regions between the ridges contain a maximum surface charge density, a maximum electric field intensity is also found in these regions. Also, the planar SPP dispersion curve (only slightly perturbed by the grating), which resides outside the light line, will have field maxima in these same regions. Therefore anticrossing may occur between the two bands, and this can be seen if, instead of plotting the reflectivities as we have

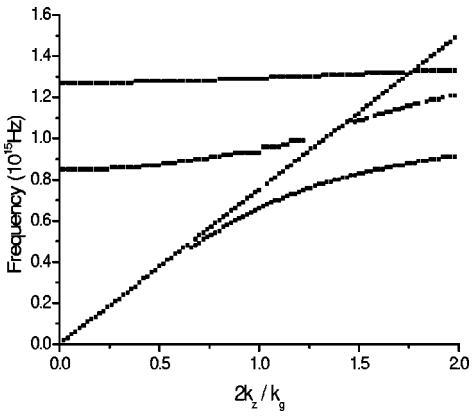

Fig. 7. Band structure for a 200-nm-pitch silver grating consisting of a series of 40-nm-wide, 50-nm-deep Gaussian ridges. The first- and second-order SPPs are shown as well as the light line and the SPP dispersion curve centered at the origin.

so far in this paper, we plot the band structure. We have done this for a 50-nm-deep grating, which resulted in the reflectivity plot of Fig. 4(a), and the band structure is shown in Fig. 7.

In Fig. 7 there are four lines: the light line (the diagonal line centered at the origin), the planar surface SPP dispersion curve (also centered at the origin), and two lines that are the first- and second-order SPPs (which originate at $f \approx 0.85 \times 10^{15}$ Hz and $f \approx 1.28 \times 10^{15}$ Hz). The peculiarity of this plot is that the planar surface SPP should approach $f \approx 1.5 \times 10^{15}$ Hz (since this is the equivalent of ω_{sp} in this plot), yet it is clearly approaching a limit at a frequency lower than this. What is in fact happening is that anticrossing is occurring between the first-order grating-coupled SPP and the "planar" surface SPP curve, so that the "planar" surface SPP curve at high values of k_z is approaching the dispersion expected of the first-order SPP, and the first-order SPP is approaching that of the "planar" surface SPP. This is the cause of the increased gradient in the first-order SPP when it is compared with the other SPP curves shown in Figs. 4(a) and 4(b). Similarly, when the higher-order grating-coupled SPPs decrease in frequency such that they cross with the lowest-order grating-coupled SPP, anticrossing may also take place, since all of these modes have strong fields on the flat regions between the ridges. This is clearly seen in Figs. 4(c) and 4(d).

4. SURFACE PLASMON POLARITONS ON NARROW-RIDGED SHORT-PITCH METAL GRATINGS AT A 45° AZIMUTHAL ANGLE

Having considered the dispersion and optical response of the Gaussian-ridged gratings at a 90° azimuthal angle, we will now consider the case of the grating oriented at a 45° azimuthal angle. In this orientation, polarization conversion can occur,[18,19] and we will consider primarily the effect of the SPPs on the polarization conversion. Since we are considering the case of an azimuthal angle of 45°, both TM- and TE-polarized light can couple to the SPP modes, and the results of considering TM-polarized incident light are much the same as considering those of TE-polarized incident light. Therefore it does not matter which we choose to investigate; we have chosen TM-polarized light.

The polarization-conserved and polarization-converted TM reflectivities for 200-nm-pitch silver gratings consisting of a series of 40-nm-wide Gaussian ridges oriented at a 45° azimuthal angle as a function of frequency and in-plane wave vector, and for various depths, are shown in Fig. 8.

The most obvious point to note in Fig. 8 is the broadband polarization conversion that occurs when the height of the grating ridges is large. This phenomenon is the focus of attention in a separate paper.[13] Here we shall concentrate on the SPP bands that are evident as relatively sharp features for nonnormal angles of incidence.

The dispersion of the SPP bands in this orientation is a result of the evolution of the SPP dispersion curves for an azimuthal angle of 0° (described in Ref. 12), to those of the SPP dispersion curves for an azimuthal angle of 90° (described earlier in this paper). The bands exist for all possible grating orientations and vary monotonically between these two limiting azimuthal angles, with the dispersion in the orientation considered here appearing slightly more like those observed for an azimuthal angle of 90°, rather than 0°.

The more interesting feature is the effect of these SPPs on the polarization conversion from the structure. For shallow gratings the polarization conversion is enhanced by the SPP, whereas for deeper gratings it is suppressed. In fact, the suppression of the polarization conversion occurs when the SPPs arise in a region of broadband polarization conversion. To understand this, we need to consider in more detail the process by which polarization conversion occurs.

Typically, SPP-mediated polarization conversion occurs because both TM- and TE-polarized light can be used to excite the SPP, and therefore both TM- and TE-polarized light may be reradiated into the specularly reflected order regardless of which polarization has been used to excite the SPP. Since at a 45° azimuthal angle the coupling into and out of the SPP mode is equal for both TM- and TE-polarized light (at normal incidence), it may be somewhat surprising that the polarization-converted reflectivity is often higher than 50% and may in fact approach nearly 100%.

To understand this, we will begin by considering the case of light incident on a shallow grating oriented at a 0° azimuthal angle. When a SPP is excited, a reflectivity minimum is produced, but we must consider where this lost energy has been dissipated. The excited SPP scatters out of the grating and into the specularly reflected order, whereupon it interferes destructively with the light that has been directly reflected from the surface. This produces the reflectivity minimum, but the energy has to have been dissipated somewhere. The only other energy-loss channel available (if the structure is nondiffractive) is absorption in the metal, and in this situation this is where the energy has been lost.

In the case of polarization conversion when the azimuthal angle is 45°, both TM- and TE-polarized light has been scattered into the specularly reflected order from the SPP. If we are considering TM-polarized incident light,

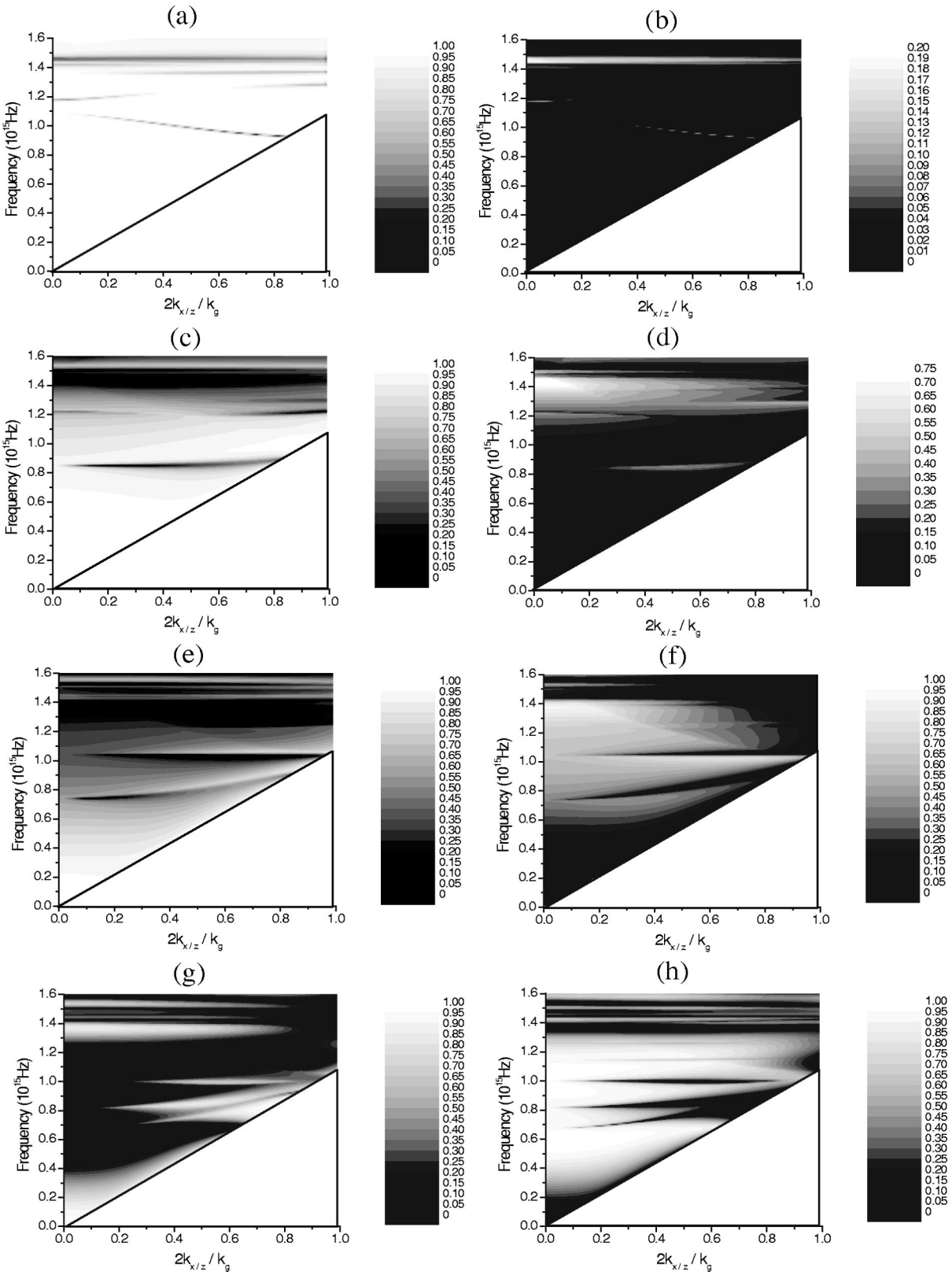

Fig. 8. Zero-order TM reflectivities for 200-nm-pitch silver gratings consisting of a series of 40-nm-wide Gaussian ridges oriented at a 45° azimuthal angle as a function of frequency and in-plane wave vector. (a) 10-nm-deep, polarization conserved; (b) 10-nm-deep, polarization converted; (c) 50-nm-deep, polarization conserved; (d) 50-nm-deep, polarization converted; (e) 100-nm-deep, polarization conserved; (f) 100-nm-deep, polarization converted; (g) 200-nm-deep, polarization conserved; (h) 200-nm-deep, polarization converted.

then the TM-polarized light scattered out of the SPP will destructively interfere with the directly reflected light as before. In this situation, however, there is an extra energy-loss channel into the polarization-converted scat-

tered light. Whether this energy is lost into absorption or the polarization-converted signal depends on the probability of scattering of the SPP from the surface. This is increased for deeper gratings, meaning that the majority of the energy will be distributed into the polarization-converted signal, and therefore the polarization conversion from the structure can approach 100%.

To explain the suppression of the polarization conversion that is due to the SPP in the plots of Fig. 8, we must again consider the energy distributions between the polarization-conserved and the polarization-converted signals. For a deep grating there is a broadband polarization-conversion region in which the SPPs are excited. If an SPP scatters into the specularly reflected order, then destructive interference will occur in the polarization-converted signal rather than the polarization-conserved signal, because the vast majority of the light in the specularly reflected signal that is not due to these SPPs is already polarization converted. There are only two energy-loss channels: absorption in the metal and redistribution into the polarization-conserved signal. The same arguments apply as before, meaning that maxima are observed in the polarization-conserved signal, which may approach 100%.

5. SUMMARY

In this paper we have extended the modeling of the optical response of deep short-pitch gratings to consider structures consisting of a series of narrow Gaussian ridges in the conical mount. In Section 1 we have considered the case of light incident when the grating is oriented at a 90° azimuthal angle. We have shown that the low-energy bands produced by bandgaps in the SPP dispersion curves can be excited only with TM-polarized light and that these may arise in the zero-order region of the spectrum. We have also explained the dispersion of these modes in terms of anticrossing between the SPP dispersion curves created by scattering from the grating and the planar surface SPP dispersion curve arising from the origin, which is relatively unperturbed by the grating.

When the grating is oriented at a 45° azimuthal angle, polarization conversion occurs, and, on deep narrow-ridged structures, broadband polarization conversion arises. The result of excitation of SPPs is to either enhance or suppress the polarization conversion depending on whether the SPP occurs in a region of this broadband polarization conversion.

ACKNOWLEDGMENTS

The authors are grateful for support from the Engineering and Physical Sciences Research Council and the provision of a Cooperative Award in Science and Engineering award by QinetiQ, Farnborough, UK, to I. R. Hooper. This research was carried out as part of Technology Group 08 of the MoD Corporate Research Fund.

The corresponding author, I. R. Hooper, may be reached at i.r.hooper@exeter.ac.uk.

REFERENCES

1. H. Raether, *Surface Plasmons on Smooth and Rough Surface and on Gratings* (Springer-Verlag, Berlin, 1988).
2. T. Lopez-Rios, F. Mendoza, F. J. Garcia-Vidal, J. Sanchez-Dehesa, and B. Pannetier, "Surface shape resonances in lamellar metallic gratings," Phys. Rev. Lett. **81**, 665–668 (1998).
3. F. J. Garcia-Vidal, J. Sanchez-Dehesa, A. Dechelette, E. Bustarret, T. Lopez-Rios, T. Fournier, and B. Pannetier, "Localized surface plasmons in lamellar metallic gratings," J. Lightwave Technol. **17**, 2191–2195 (1999).
4. J. A. Porto, F. J. Garcia-Vidal, and J. B. Pendry, "Transmission resonances on metallic gratings with very narrow slits," Phys. Rev. Lett. **83**, 2845–2848 (1999).
5. T. W. Ebbesen, H. J. Lezec, H. F. Ghaemi, T. Thio, and P. A. Wolff, "Extraordinary optical transmission through subwavelength hole arrays," Nature (London) **391**, 667–669 (1998).
6. H. F. Ghaemi, T. Thio, D. E. Grupp, T. W. Ebbesen, and H. J. Lezec, "Surface plasmons enhance optical transmission through subwavelength holes," Phys. Rev. B **58**, 6779–6782 (1998).
7. L. Salomon, F. D. Grillot, A. V. Zayats, and F. de Fornel, "Near-field distribution of optical transmission of periodic subwavelength holes in a metal film," Phys. Rev. Lett. **86**, 1110–1113 (2001).
8. L. Martin-Moreno, F. J. Garcia-Vidal, H. J. Lezec, K. M. Pellerin, T. Thio, J. B. Pendry, and T. W. Ebbesen, "Theory of extraordinary optical transmission through subwavelength hole arrays," Phys. Rev. Lett. **86**, 1114–1117 (2001).
9. M. B. Sobnack, W. C. Tan, N. P. Wanstall, T. W. Preist, and J. R. Sambles, "Stationary surface plasmons on a zero-order metal grating," Phys. Rev. Lett. **80**, 5667–5670 (1998).
10. W. C. Tan, T. W. Preist, J. R. Sambles, and N. P. Wanstall, "Flat surface-plasmon-polariton band and resonant optical absorption on short-pitch metal gratings," Phys. Rev. B **59**, 12661–12666 (1999).
11. I. R. Hooper and J. R. Sambles, "Dispersion of surface plasmon polaritons on short-pitch metal gratings," Phys. Rev. B **65**, 165432 (2002).
12. I. R. Hooper and J. R. Sambles, "Surface plasmon polaritons on narrow-ridged short-pitch metal gratings," Phys. Rev. B **66**, 205408 (2002).
13. I. R. Hooper and J. R. Sambles, "A broadband polarization converting mirror for the visible region of the spectrum," Opt. Lett. **27**, 2152–2154 (2002).
14. N. P. K. Cotter, T. W. Preist, and J. R. Sambles, "Scattering-matrix approach to multilayer diffraction," J. Opt. Soc. Am. A **12**, 1097–1103 (1995).
15. J. Chandezon, M. T. Dupuis, G. Cornet, and D. Maystre, "Multicoated gratings—a differential formalism applicable in the entire optical region," J. Opt. Soc. Am. **72**, 839–846 (1982).
16. R. A. Watts, T. W. Preist, and J. R. Sambles, "Sharp surface-plasmon resonances on deep diffraction gratings," Phys. Rev. Lett. **79**, 3978–3981 (1997).
17. W. L. Barnes, T. W. Preist, S. C. Kitson, and J. R. Sambles, "Physical origin of photonic energy gaps in the propagation of surface plasmons on gratings," Phys. Rev. B **54**, 6227–6224 (1996).
18. S. J. Elston, G. P. Bryan-Brown, and J. R. Sambles, "Polarization conversion from diffraction gratings," Phys. Rev. B **44**, 6393–6400 (1991).
19. R. A. Depine and M. Lester, "Internal symmetries in conical diffraction from metallic gratings," J. Mod. Opt. **48**, 1405–1411 (2001).